Supporting Information

Porous Au@Pt Nanoparticles: Therapeutic Platform for Tumor Chemo-Photothermal Co-Therapy and Alleviating Doxorubicin-Induced Oxidative Damage

Qian Yang[§], *Jinrong Peng*[†], *Yao Xiao*[†], *Wenting Li*[‡], *Liwei Tan*[#], *Xiaohong Xu*[§], *Zhiyong Qian*[†,*]

[†] State Key Laboratory of Biotherapy, West China Hospital, and Collaborative Innovation Center of Biotherapy, Sichuan University, No. 17, Section 3, Southern Renmin Road, Chengdu 610041, Sichuan, P. R. China

[§] School of Pharmacy, College Key Laboratory of Sichuan Province for Specific Structure of Small Molecule Drugs, Chengdu Medical College, No. 783, Xindu Avenue, Xindu District, Chengdu 610500, Sichuan, P. R. China

[‡] Department of Pharmacy, West China Second University Hospital, Chengdu 610041, Sichuan, P. R. China

[#] College of Medicine, Southwest Jiaotong University, Chengdu 610031, Sichuan, P.R. China

Corresponding Author

* E-mail: anderson-qian@163.com

Table S1 The Au and Pt Contents Measured by ICP-MS

Samples	Au, % (w/w)	Pt, % (w/w)
Au@Pt-40	57.3±0.68	42.6±0.28
Au@Pt-60	60.2±1.2	39.6±0.26
Au@Pt-100	62.1±1.8	37.4±0.34

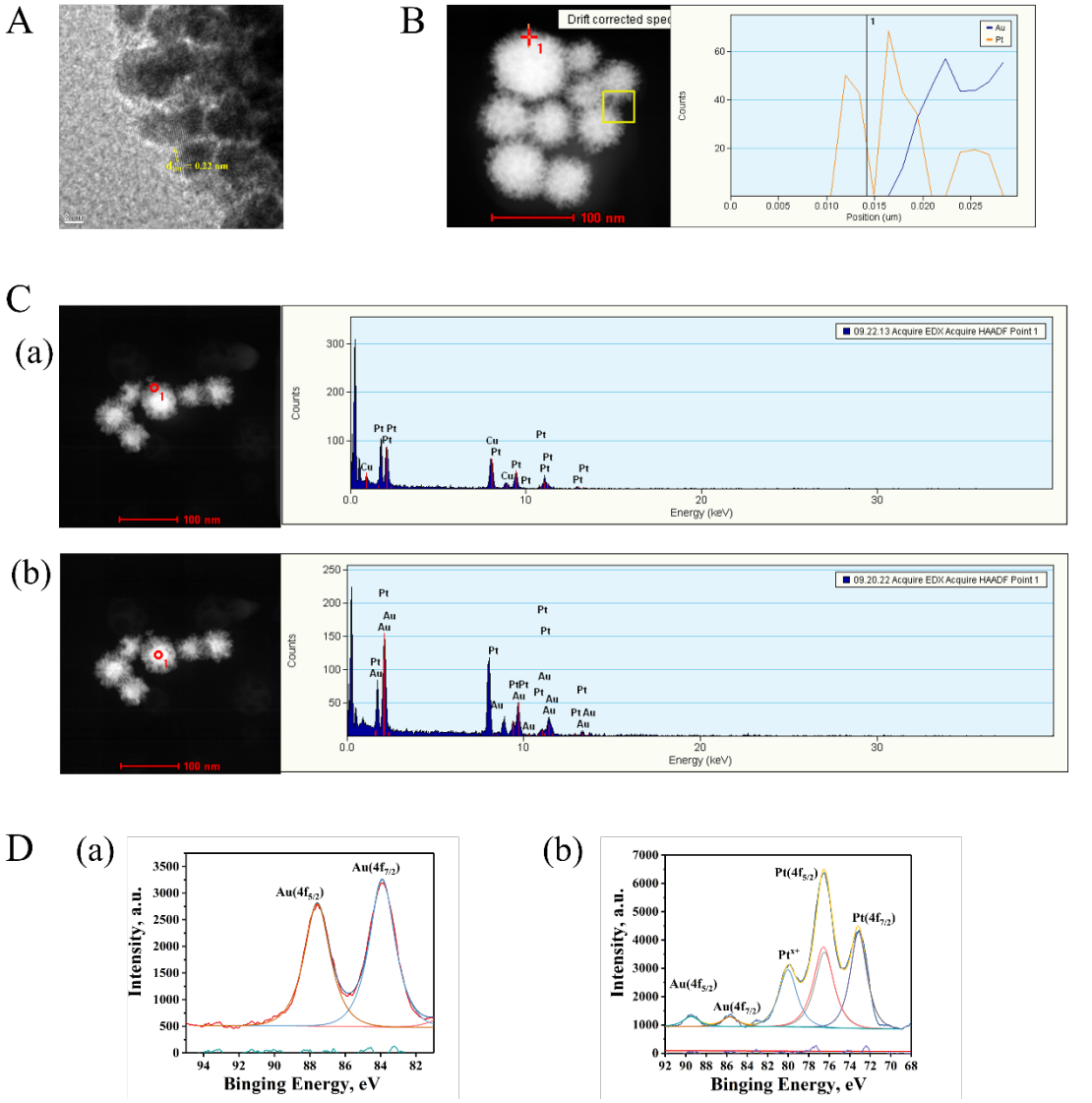

Figure S1. (A) HRTEM image of Au@Pt. (B) STEM-EDX line profiles of Au@Pt nanoparticles. (C) EDX analysis of (a) the edge and (b) the middle of composite Au@Pt nanoparticles. (D) X-ray photoelectron spectroscopy (XPS) analysis of Au and Au@Pt nanocparticles: (a) XPS spectra of Au nanocparticles, (b) XPS spectra of Au@Pt Au nanocparticles.

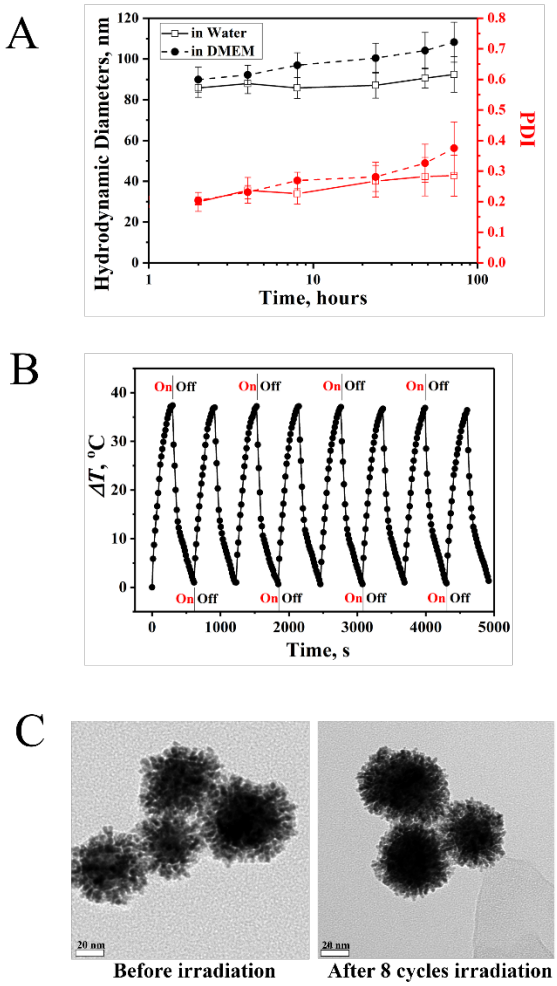

Figure S2. (A) The stability of DOX/Au@Pt-cRGD in medium of water and DMEM, respectively. (B) Photothermal conversion of DOX/Au@Pt-cRGD in aqueous solution (50 μg/mL) over eight ON/OFF cycles of 808 nm laser (laser power: 1.5W/cm^2). (C) The TEM imaging of DOX/Au@Pt-cRGD nanoparticles before and after irradiation.

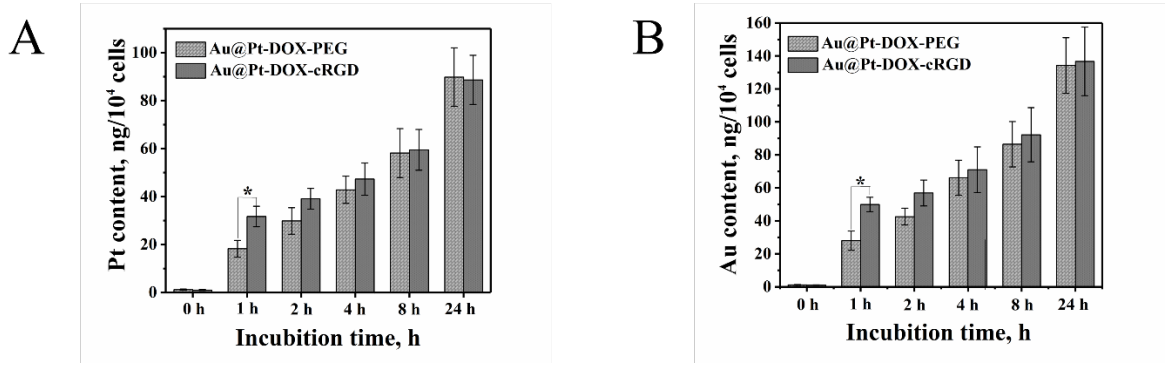

Figure S3. (A and B) Pt and Au contents in MDA-MB-231 cells after incubation with DOX/Au@Pt-PEG and DOX/Au@Pt-cRGD for different time point. Data displayed as mean ± SD (n = 3)

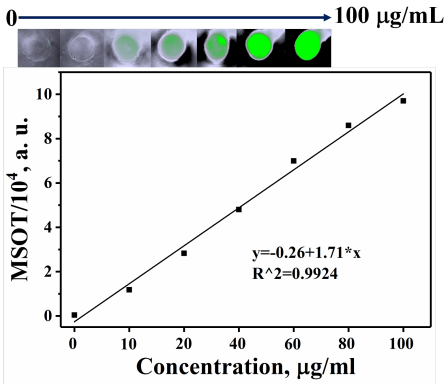

Figure S4. The linear association of Au@Pt concentration and MSOT intensity of PA signal acquired from phantom at 680 nm.

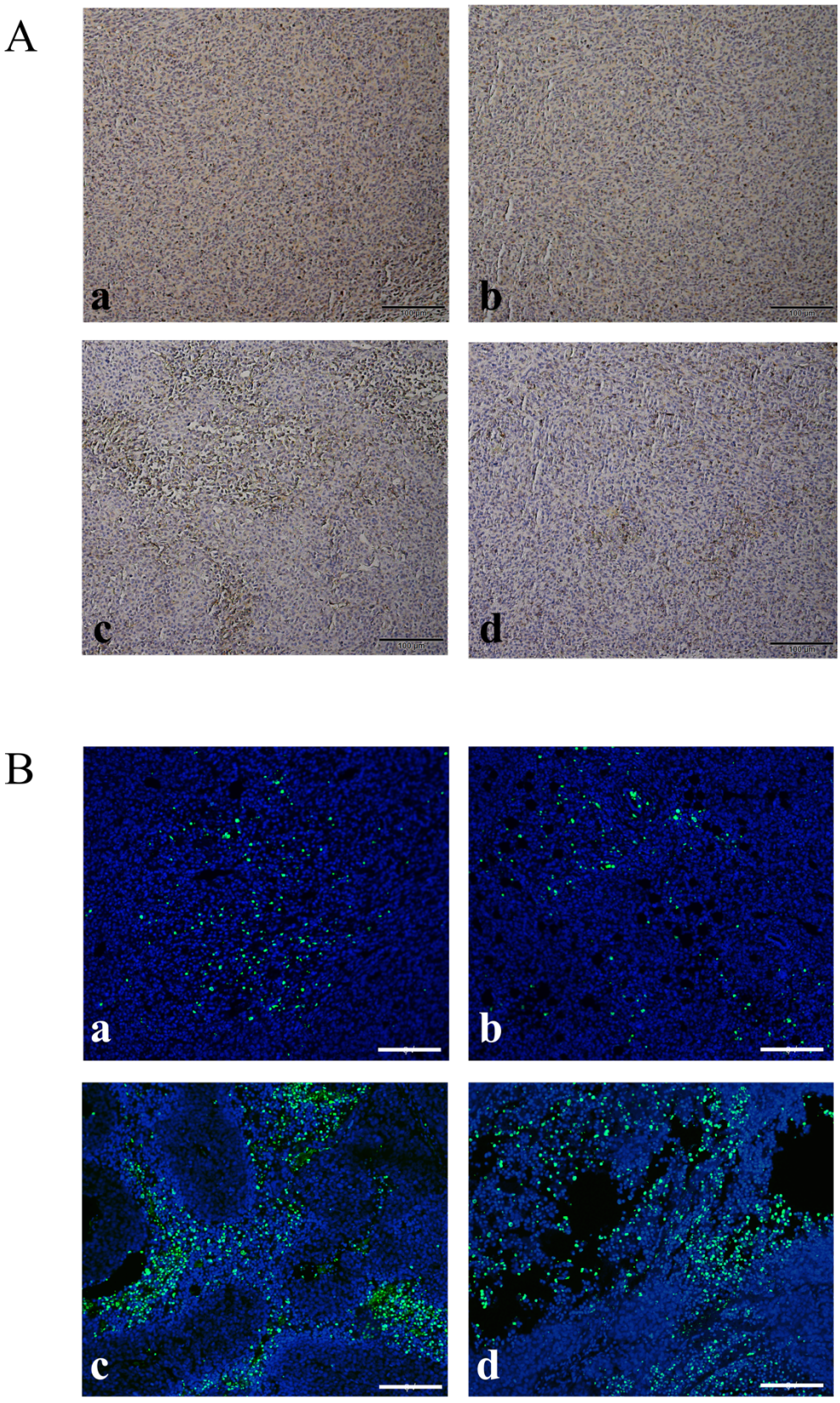

Figure S5. Representative enlarged imagings of Ki-67 and TUNEL staining for MDA-MB-231 tumor (Treatments: a. free DOX, b. DOX/Au@Pt-cRGD, c. Au@Pt-cRGD+Laser, d. DOX/Au@Pt-cRGD+Laser): (A) immunohistochemical staining of Ki-67. (B) immunoflourescent staining of TUNEL (Scale bar = 100 μm).

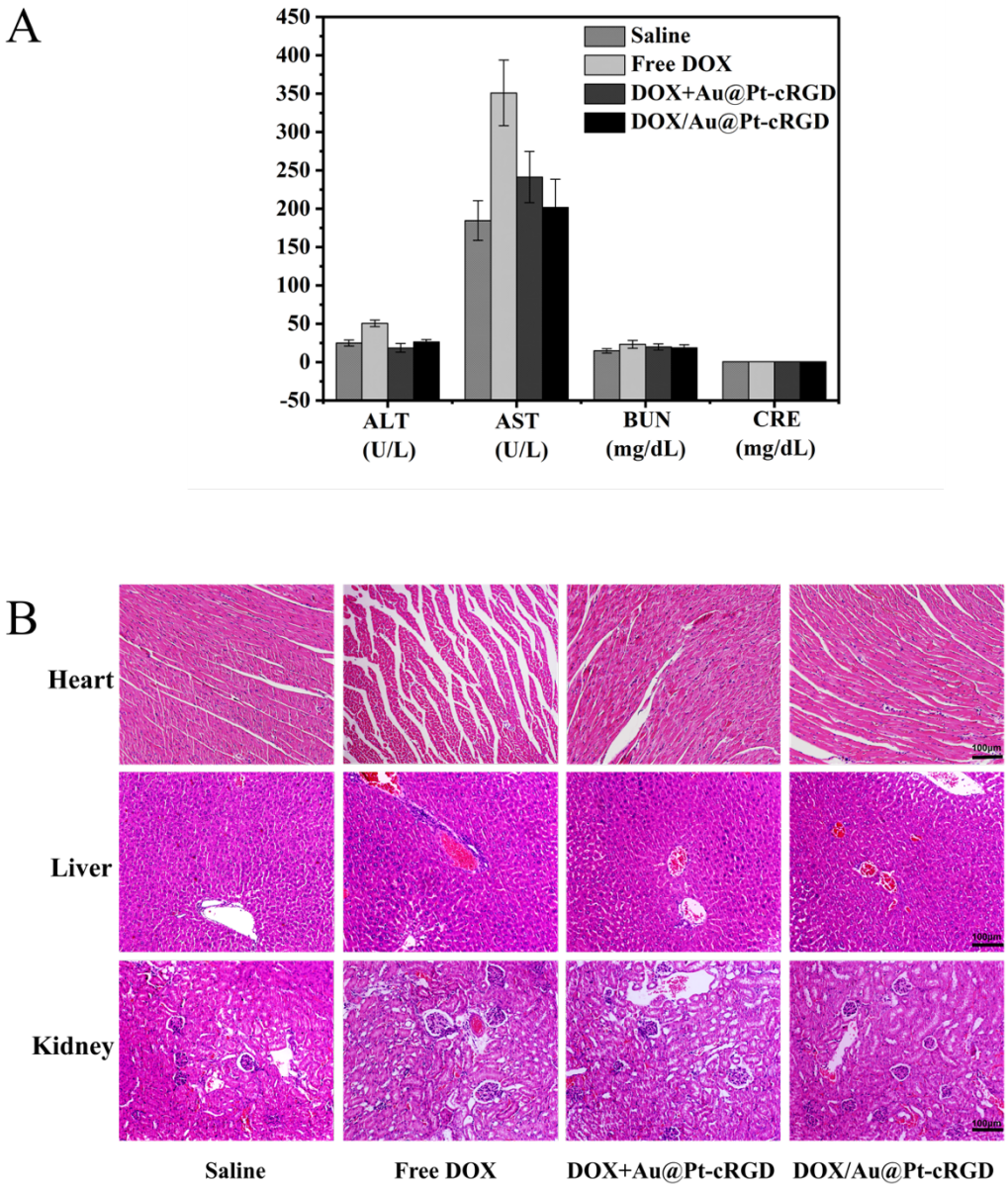

Figure S6. (A) Biochemical assays of liver and kidney function following a 10-day treatment course, Data displayed as mean ± SD (n = 3). (B) Representative H&E stained images of the heart, liver, and kidney tissues in each group (Scale bar = 100 μm).